EBioMedicine 47 (2019) 142–155

Contents lists available at ScienceDirect

EBioMedicine

journal homepage: www.ebiomedicine.com

EBioMedicine
Published by THE LANCET

Annexin10 promotes extrahepatic cholangiocarcinoma metastasis by facilitating EMT via PLA2G4A/PGE2/STAT3 pathway

Rongqi Sun [a,1], Zengli Liu [a,1], Bo Qiu [a], Tianli Chen [a], Zhipeng Li [b], Xiaoming Zhang [a], Yunfei Xu [a,*], Zongli Zhang [a,*]

[a] Department of General Surgery, Qilu Hospital of Shandong University, Jinan, China
[b] Department of General Surgery, Shandong Provincial Hospital, Jinan, China

ARTICLE INFO

Article history:
Received 22 June 2019
Received in revised form 22 August 2019
Accepted 26 August 2019
Available online 3 September 2019

Keywords:
Annexin 10
Perihilar cholangiocarcinoma
Distal cholangiocarcinoma
Prognosis
Metastasis
Epithelial-mesenchymal transition

ABSTRACT

Background: Cholangiocarcinoma (CCA), consisting of intrahepatic (IHCCA), perihilar (PHCCA), and distal (DCCA) CCA, is a type of highly aggressive malignancy with a very dismal prognosis. Potential biomarkers and drug targets of CCA are urgently needed. As a new member of the Annexin (ANXA) family, the role of ANXA10 in the progression and prognosis of CCA is unknown.

Methods: Potential PHCCA biomarkers were screened by transcriptome sequencing of 5 pairs of PHCCA and adjacent tissues. The clinical significance of ANXA10 was evaluated by analyzing its correlation with clinicopathological variables, and the prognostic value of ANXA10 was evaluated with univariate and multivariate analyses. The function of ANXA10 in the epithelial-mesenchymal transition (EMT), proliferation, invasion and metastasis was detected with in vitro and in vivo experiments. Moreover, we screened the key molecule in ANXA10-induced CCA progression by mRNA sequencing and evaluated the correlation between PLA2G4A and ANXA10. The effect of PLA2G4A downstream signaling, including Cyclooxygenase 2, Prostaglandin E2(PGE2) and Signal transducer and activator of transcription 3(STAT3), on EMT and metastasis was further detected with in vitro and in vivo experiments.

Findings: ANXA10 expression was upregulated in PHCCA and DCCA but not in IHCCA. High ANXA10 expression was significantly associated with poor tumor differentiation and prognosis. ANXA10 promoted the proliferation, migration and invasion of the PHCCA cells. PLA2G4A expression was regulated by ANXA10 and high PLA2G4A predicted poor prognosis in PHCCA and DCCA. ANXA10 facilitated EMT and promoted metastasis by upregulating PLA2G4A expression, thus increasing PGE2 levels and activating STAT3.

Interpretation: ANXA10 was an independent prognostic biomarker of PHCCA and DCCA but not IHCCA. ANXA10 promoted the progression of PHCCA and facilitated metastasis by promoting the EMT process via the PLA2G4A/PGE2/STAT3 pathway. ANXA10, PLA2G4A and their downstream molecules, such as COX2 and PGE2, may be promising drug targets of PHCCA and DCCA.

1. Introduction

Cholangiocarcinoma (CCA) is a malignant tumor originating from the biliary epithelium [1]. For a long time, CCA was classified into intrahepatic CCA (ICCA) and extrahepatic CCA (EHCCA) according to its anatomical location until the 7th AJCC/UICC staging system in 2007, which further categorized CCA as three subtypes: intrahepatic (ICCA), perihilar (PHCCA), and distal (DCCA) CCA [2]. This is a milestone in the study of CCA because it confirmed that each subtype has a distinct epidemiology, biology, prognosis, and strategy for clinical management [3,4]. PHCCA, also known as Klatskin's tumor, is the most common subtype and accounts for 50–70% of all CCA, while DCCA and ICCA account for approximately 20–30% and 10%, respectively [5]. Radical surgery is the main curative treatment for CCA, but ICCA, PHCCA and DCCA have

Abbreviations: CCA, cholangiocarcinoma; PHCCA, perihilar cholangiocarcinoma; ICCA, intrahepatic cholangiocarcinoma; DCCA, distal cholangiocarcinoma; AJCC/UICC, American Joint Committee on Cancer/Union for International Cancer Control; TMA, tissue microarray; OS, overall survival; FBS, fetal bovine serum; PBS, phosphate-buffered saline; IHC, immunohistochemistry; SDS-PAGE, sodium dodecyl sulfate polyacrylamide gel electrophoresis; PVDF, polyvinylidene fluoride; qRT-PCR, quantitative real-time PCR; CCK-8, cell counting kit-8; FACS, fluorescence-activated cell sorting; ANXA, annexin; EMT, epithelial-mesenchymal transition; PLA2G4A, Cytosolic phospholipase A2; PGE2, Prostaglandin E2; AA, arachidonic acid; COX2, Cyclooxygenase-2; Snail, Zinc finger protein SNAIl; STAT3, Signal transducer and activator of transcription 3.

* Corresponding authors at: Department of General Surgery, Qilu Hospital of Shandong University, 107 Wenhua Road, Jinan, Shandong 250012, China.
E-mail addresses: xuyunfei1988@126.com (Y. Xu), zzlzzl1900@163.com (Z. Zhang).
[1] Means these authors contribute equally.

https://doi.org/10.1016/j.ebiom.2019.08.062

Research in context

Evidence before this study

Cholangiocarcinoma(CCA) is a type of highly aggressive malignancy with no well-accepted target therapies. CCA can be further categorized CCA as intrahepatic (ICCA), perihilar (PHCCA), and distal (DCCA) CCA, which have a distinct epidemiology, biology, prognosis, and strategy for clinical management. The prognosis of CCA is very poor and there is still no targeted drug available for CCA in the era of personalized treatment. The clinical trials, preclinical drugs and studies of potential biomarkers of CCA lag far behind other tumors like lung cancer.

Added value of this study

In our study, we screened potential biomarkers with exome and transcriptome sequencing, and first demonstrated that ANXA10 is an independent prognostic biomarker of PHCCA and DCCA. After various in vitro and in vivo experiments, we suggested that PLA2G4A expression was regulated by ANXA10 and that it is essential for ANXA10-induced proliferation, invasion and EMT in CCA, and PGE2 generation and STAT3 activation downstream of PLA2G4A were essential in ANXA10-mediated EMT facilitation and tumor metastasis.

Implications of all the available evidence

Our results may help stratify high-risk patients with PHCCA and DCCA and guide individualized treatment for PHCCA and DCCA. Our findings suggested that ANXA10, PLA2G4A and COX-2 are potential drug targets for PHCCA and DCCA, and drugs blocking the ANXA10/PLA2G4A/PGE2 pathway such as Celecoxib are a promising therapeutic approaches for CCA treatment.

completely different surgical approaches for curative treatment. Hepatectomy is the main approach for ICCA, while DCCA patients usually need to undergo local resection or pancreatoduodenectomy [6]. Surgical treatment for PHCCA is more complicated and technically challenging because of the complex, intimate and variable relationship between biliary and vascular structures at the hepatic portal [7]. Moreover, most patients with CCA have often lost their opportunity for radical surgery upon first diagnosis due to silent clinical symptoms and rapid progression [8]. Furthermore, the effects of adjuvant therapy for CCA, including chemotherapy and radiotherapy, are unsatisfactory. All of the above reasons contribute to the poor prognosis for CCA and its 5-year overall survival rate of approximately 30% after radical surgery [8]. Unfortunately, there is still no targeted drug available for CCA in the era of personalized treatment [9]. This predicament is more severe for PHCCA and DCCA because the clinical trials, preclinical drugs and studies of potential biomarkers for PHCCA and DCCA all lag far behind ICCA [10].

The Annexin family is the largest category of eukaryotic calcium and phospholipid-binding proteins and plays important roles in various physiological processes, including cell differentiation and proliferation [11]. The Annexin A (ANXA) subclass contains 12 members in humans [12], and the ectopic expression of the ANXA members was observed in the tumorigenesis and progression of several types of cancers, such as the up-regulation of ANXA1 in pancreatic cancer [13]. Interestingly, tumor growth and metastasis are significantly decreased in AnxA1-KO mice, indicating a critical role of ANXA1 in tumor progression [14]. However, different ANXA members play different roles in cancer progression. For example, downregulation of ANXA members was reported in certain types of tumors, such as low expression of ANXA1 and ANXA7 in prostatic cancer [15]. Moreover, the expression and function of ANXA in cancer are tissue-specific or context-specific. From the exome and transcription sequencing of PHCCA, we found that ANXA10 was upregulated in PHCCA tissues. However, as a new member of the Annexin family, the role of ANXA10 in cancer progression has rarely been investigated, and understanding its expression and function in CCA requires more experiments.

Tumor-associated chronic inflammation is a hallmark of cancer that facilitates progression to a metastatic stage. The longstanding inflammation and injury such as primary sclerosing cholangitis, bile duct calculus is a well-known risk of CCA [16,17]. In the process of inflammation, phospholipase A2 (PLA2) is a group of key enzymes that cleave phospholipids specifically at the sn-2 position to liberate free fatty acids, mostly arachidonic acid (AA) and lysophospholipids (LPLs). PLA2 can be divided mainly into secretory PLA2s (sPLA2), cytosolic PLA2s (cPLA2), calcium-independent PLA2s (iPLA2) and other isoforms according to their location. As the main type of PLA2, cPLA2a, also known as group IVA cPLA2 (PLA2G4A), can help convert arachidonic acid to a variety of eicosanoids, mainly prostaglandin E2 (PGE2) in the presence of cyclooxygenase (COX) enzymes. In this way, cPLA2 is involved in many physiological and pathological processes, including inflammation, cell growth, invasion and metastasis. Among the ANXA family, ANXA1 is a relatively well-studied member. ANXA1 was previously reported to suppress inflammation by inhibiting the activity of cPLA2 and interfering with AA release [18,19]. However, whether other ANXA members regulate cPLA2 activity or expression and whether cPLA2 is involved in the progression of CCA is unknown.

Here, in our study, we first screened possible biomarkers of CCA by exome and transcription sequencing of 5 pairs of PHCCA and adjacent tissues and verified the upregulation and prognostic significance of ANXA10 in PHCCA and DCCA but not in ICCA. Through in vitro and in vivo experiments, we investigated the role of ANXA10 in CCA progression. Moreover, we screened the key molecule involved in ANXA10-induced progression by mRNA sequencing and found that cPLA2a expression was regulated by ANXA10. To reveal the correlations among ANXA10, cPLA2a and CCA progression, we further studied the molecular mechanism of how cPLA2 influenced CCA progression and prognosis.

2. Materials and methods

2.1. Patients and follow-up

The primary cohort comprised patients who underwent surgery for ICCA (254 cases), PHCCA (374 cases) and DCCA (231 cases) at Qilu Hospital of Shandong University from 2012 to 2018. A validation cohort consisting of 91 ICCA patients, 128 PHCCA patients and 84 DCCA patients was further selected according to the following inclusion criteria: (i) patients who underwent radical resection with a clear surgical margin; (ii) patients with available formalin-fixed tumor tissues, follow-up information and complete medical records; (iii) patients with a postsurgical survival time of >1 month; and (iv) patients with no history of other malignancies. Twenty pairs of ICCA, PHCCA, and DCCA and tumor-adjacent normal tissues were collected continuously during operations on the premise of not interfering with the pathological diagnosis. The tumors were classified and staged according to the 7th AJCC/UICC TNM classification system.

2.2. Ethics statement

Informed consent was obtained from all patients. All experiments were approved and supervised by the Ethics Committee of Qilu Hospital of Shandong University.

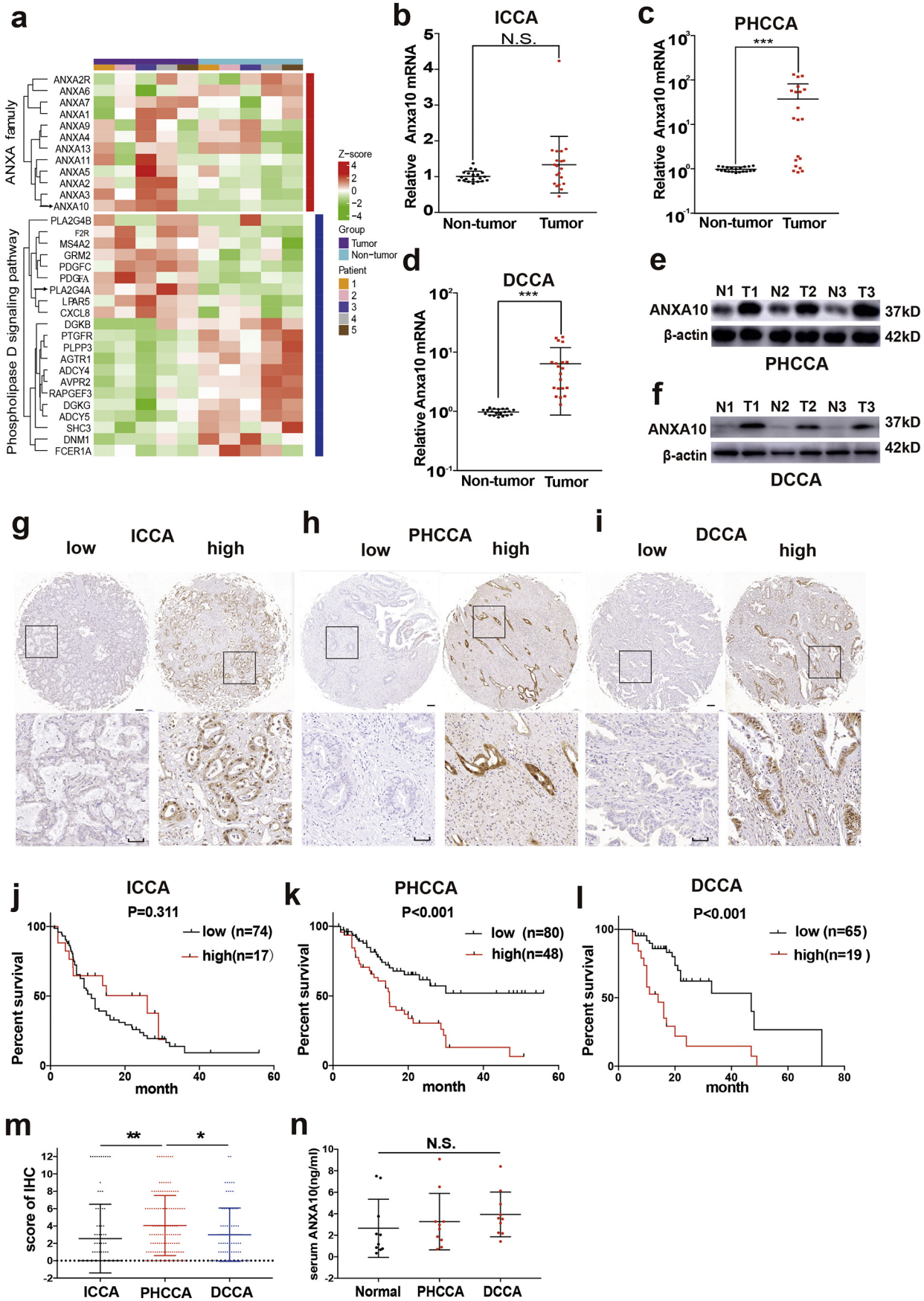
a
ANXA famuly
ANXA2R
ANXA6
ANXA7
ANXA1
ANXA9
ANXA4
ANXA13
ANXA11
ANXA5
ANXA2
ANXA3
ANXA10
Phospholipase D signaling pathway
PLA2G4B
F2R
MS4A2
GRM2
PDGFC
PDGFA
PLA2G4A
LPAR5
CXCL8
DGKB
PTGFR
PLPP3
AGTR1
ADCY4
AVPR2
RAPGEF3
DGKG
ADCY5
SHC3
DNM1
FCER1A
Z-score
Group
Tumor
Non-tumor
Patient
b
ICCA
N.S.
Relative Anxa10 mRNA
Non-tumor
Tumor
c
PHCCA
***
Relative Anxa10 mRNA
Non-tumor
Tumor
d
DCCA
***
Relative Anxa10 mRNA
Non-tumor
Tumor
e
N1 T1 N2 T2 N3 T3
ANXA10
β-actin
37kD
42kD
PHCCA
f
N1 T1 N2 T2 N3 T3
ANXA10
β-actin
37kD
42kD
DCCA
g
low
ICCA
high
h
low
PHCCA
high
i
low
DCCA
high
j
ICCA
P=0.311
low (n=74)
high(n=17)
Percent survival
month
k
PHCCA
P<0.001
low (n=80)
high(n=48)
Percent survival
month
l
DCCA
P<0.001
low (n=65)
high(n=19)
Percent survival
month
m
**
*
score of IHC
ICCA
PHCCA
DCCA
n
N.S.
serum ANXA10(ng/ml)
Normal
PHCCA
DCCA

2.3. Agents and cells

Human PHCCA cell lines QBC-939 and FRH-0201 and IHCCA cell lines RBE and HCCC-9810 were all purchased from the Cell Bank of the Chinese Academy of Sciences (Shanghai, China). All cell lines were maintained in DMEM (Gibco, Grand Island, New York, USA) supplemented with 10% fetal bovine serum (Gibco) and penicillin/streptomycin (HyClone) in 5% CO_2. All cell lines were authenticated using short tandem repeat (STR) analysis, and the databases of the Chinese Academy of Sciences and American Type Culture Collection were used as references.

The inhibitors AACOCF3 (APExBIO) and celecoxib (Selleck, Houston, TX, USA) were used. All other agents without special instructions were purchased from Sigma. The information for the antibodies is detailed as follows: ANXA10(Sigma-Aldrich, St. Louis, MS, United States, C114395),Snail(Cell Signaling Technology, Danvers, MA, #3879), Vimentin(Cell Signaling Technology, #5741), E-cadherin(Cell Signaling Technology, #3195), PLA2G4A(Abcam, Cambridge, UK, ab58375), GNA13(Abcam, ab128900), STAT3(Abcam, ab68153), Phospho-Stat3-Tyr705(Cell Signaling Technolog, #9145).

2.4. Tissue microarray and IHC

Tissue microarray (TMA) was constructed using paraffin-embedded sections of tumors after hematoxylin and eosin staining to confirm the representative tumor area. Core tissues with a 1.5-mm diameter were used for TMA construction. Immunohistochemistry (IHC) was performed on the TMA slides for the detection of ANXA10 or PLA2G4A, as detailed in a previous study [20]. In brief, the slides were submerged in EDTA (pH = 9) buffer for optimal antigen retrieval. Primary ANXA10 antibody (1:500) or anti-PLA2G4A antibody (1:400) was applied and incubated with the specimens at 4 °C overnight. A biotin-labeled goat anti-rabbit antibody (Zsbio, Beijing, China) was applied for 30 min at room temperature. Subsequently, the slides were incubated with conjugated horseradish peroxidase streptavidin. The peroxidase reaction was developed using a 3,3-diaminobenzidine (DAB) solution (Zsbio).

The IHC results were evaluated independently by two senior pathologists who were unaware of the clinical information. The IHC results were semi-quantitatively scored in a conventional way based on the staining intensity (0, negative; 1, weak; 2, moderate; 3, strong) and the percentage of positively stained cells (0, 0%; 1, 1%–25%; 2, 25%–50%; 3, 50%–75%; 4, 75%–100%) [21]. The final score was the product of the two scores multiplied together. The cut-off was identified as the point with the highest sum of specificity and sensitivity in the ROC curve according to a previous study [22]. The cut-offs for ANXA10 in IHCCA, PHCCA and DCCA were 5.0, 5.0 and 5.0, respectively, and the cut-offs for PLA2G4A in PHCCA and DCCA were 5.0 and 3.5, respectively.

2.5. RNA extraction and quantitative real-time PCR

Detailed in supplemental materials.

2.6. Whole-exome and mRNA sequencing

Detailed in supplemental materials.

2.7. Western blotting analysis

Detailed in supplemental materials.

2.8. ELISA assay

Detailed in supplemental materials.

2.9. Transfection and stable cell line

Detailed in supplemental materials.

2.10. CCK-8 assay

Detailed in supplemental materials

2.11. Cell cycle and apoptosis assays

Detailed in supplemental materials.

2.12. Wound healing assay

Detailed in supplemental materials.

2.13. Transwell assay

Detailed in supplemental materials.

2.14. In vivo assay

Detailed in supplemental materials.

2.15. Statistical analysis

All values are represented as the mean ± standard deviation. SPSS 17.0 and GraphPad Prism 5.0 software were used to calculate the statistical analyses and make diagrams. The correlations between ANXA10 and clinicopathological characteristics were assessed by the χ^2 or Fisher test. Survival curves were plotted using the Kaplan-Meier method, and statistical significance was compared using the log-rank test. The significant variables in univariate survival analyses were included in the final multivariable Cox proportional hazards regression model. Student's *t*-test was used for comparisons of two independent groups, and one-way ANOVA was used to compare multiple groups. *P* values <.05 were considered statistically significant.

Fig. 1. Expression and prognostic significance of ANXA10 in CCA. (a) Heatmap of altered genes in the ANXA family and phospholipase D signaling pathway in PHCCA. Dysregulated mRNAs in 5 pairs of PHCCA tissues and tumor-adjacent tissues were identified from transcriptome sequencing by hierarchical clustering. High and low expression levels are indicated in red and green, respectively. (b–d) Relative mRNA expression of ANXA10 was quantified by qRT-PCR for 20 cases of ICCA PHCCA and DCCA and their patient-paired normal tissues. The results were analyzed using the $2^{-\Delta\Delta CT}$ method with GAPDH as a reference gene. Statistical significance between groups was assessed using paired *t*-test. N.S. represents not significant, and *** represents $P < .001$. (e–f) ANXA10 protein expression was detected by western blot in 3 paired PHCCA and DCCA tissue samples. (g–i) Representative images of immunohistochemical staining for ANXA10 in ICCA, PHCCA and DCCA in the tissue microarray. Scale bar: 50 μm. (j–l) The overall survival curves of patients with ICCA, PHCCA and DCCA were stratified by ANXA10 expression. (m) IHC scores for ANXA10 in ICCA, PHCCA and DCCA. (n) Serum ANXA10 levels in 10 healthy subjects, 10 PHCCA patients and 10 DCCA patients were tested by ELISADCCA. In M and N, statistical significance between two groups was assessed using Student's *t*-test. N.S. represents not significant.

Table 1
Univariate and multivariate analysis of prognostic factors for overall survival in PHCCA and DCCA.

Variables	PHCCA					DCCA				
	Univariate analysis		Multivariate analysis			Univariate analysis		Multivariate analysis		
	3-year OS%	P*	HR	95%CI	P**	3-year OS %	P*	HR	95%CI	P**
Age(<60 vs.. ≥60)	36.2 vs. 30.1	0.566				55.8 vs. 38.7	0.086	1.59	0.68–3.75	0.286
Gender(Male vs. Female)	37.9 vs. 25.5	0.538				36.1 vs. 60.6	0.441			
Differentitation (Well vs. Moderately or Poorly)	52.2 vs. 30.4	0.113	1.75	0.70–4.40	0.235	46.3 vs. 42.5	0.246			
Tumor size (<3 cm vs. ≥3 cm)	33.6 vs. 32.7	0.250				40.1 vs. 41.1	0.078	1.13	0.54–2.34	0.747
T stages(T1–2 vs. T3–4)	33.4 vs. 32.0	0.520				50.8 vs. 34.8	0.472			
Lymph node metastasis(N0 vs. N1)	41.7 vs. 14.5	0.036	1.53	0.89–2.65	0.126	48.3 vs. 28.9	0.019	2.00	1.01–3.98	0.048
Distant metastasis(M0 vs. M1)	33.5 vs. 0	0.002	8.53	1.06–68.8	0.044	43.6 vs. 0	0.079	0.99	0.08–11.85	0.991
TNM stages(I-II vs. III-IV)	43.7 vs. 16.9	0.001				48.3 vs. 28.9	0.019			
ANXA10 (Low vs. High)	52.0 vs. 13.1	<0.001	2.25	1.31–3.84	0.026	53.3 vs. 14.6	<0.001	3.20	1.54–6.68	0.002

Abbreviations: HR = hazard ratio; 95%CI = 95% confidence interval;
* Calculated by log-rank test.
** Calculated by Cox-regression Hazard model.

3. Results

3.1. High ANXA10 expression predicts poor prognosis in PHCCA and DCCA but not in ICCA

Potential biomarkers were first screened by exome and transcriptome sequencing with five paired frozen PHCCA tissues and adjacent normal bile duct tissues (NCBI SRA under BioProject accession PRJNA517030 and PRJNA547373). According to the sequencing results, we found that ANXA10 expression was significantly higher in PHCCA tissues than in tumor-adjacent tissues (Fig. 1a). The mRNA levels of ANXA10 in 20 ICCA, PHCCA, DCCA tissues and their patient-paired normal tissues were detected with qRT-PCR (Fig. 1b–d). ANXA10 mRNA levels were remarkably higher in PHCCA and DCCA tissues than in tumor-adjacent tissues, but this tendency was not notable in ICCA tissues. Moreover, the expression of ANXA10 in another 3 pairs of PHCCA, DCCA and adjacent tissues was detected by western blotting, which also indicated the higher ANXA10 expression in PHCCA and DCCA tissues than in normal bile duct tissues (Fig. 1e and f).

Moreover, ANXA10 expression in a retrospective cohort comprising 91 ICCA patients, 128 PHCCA patients and 84 DCCA patients was detected with immunohistochemistry (IHC) (Fig. 1g–i). Interestingly, although ANXA10 is a membrane protein, the expression of ANXA10 was observed in both the nucleus and the cytoplasm. These patients were divided into low expression and high expression groups based on their IHC score for ANXA10, and the overall survival rates of patients with different ANXA10 expression were compared (Fig. 1j–l). In PHCCA and DCCA patients but not ICCA patients, high ANXA10 expression was remarkably associated with unfavorable prognosis, indicating that ANXA10 had different functions in PHCCA/DCCA and ICCA. Among ICCA, PHCCA and DCCA patients, PHCCA patients had the highest expression of ANXA10 (Fig. 1m). However, the ANXA10 level in serum was not substantially different between patients with ICCA, PHCCA, or DCCA and healthy subjects (Fig. 1n).

3.2. Clinical significance of ANXA10 in CCA

To determine the possible mechanism underlying ANXA10-involved CCA progression, we analyzed the correlation between ANXA10 and the clinicopathological features of PHCCA and DCCA patients. In both PHCCA and DCCA patients, higher ANXA10 expression was significantly associated with poorer differentiation (Supplemental Table S2). In addition, univariate and multivariate analyses were performed to evaluate the prognostic value of ANXA10 and other clinicopathological factors (Table 1). In PHCCA patients, positive lymph node metastasis ($P = .036$, log-rank test), distant metastasis ($P = .002$) and advanced TNM stage ($P = .001$) were all significantly associated with a low overall survival rate(Supplemental Fig. S1a-S1c). In DCCA patients, lymph node metastasis ($P = .019$) and TNM stage (P = .019) had a strong correlation with prognosis (Supplemental Fig. S1d-1e). Multivariate analysis with a Cox regression model was also performed to identify the independent prognostic factors of PHCCA and DCCA. Factors with a P value<.2 were enrolled in the multivariate analysis, except for TNM stage because of its natural interaction with other factors. In both PHCCA and DCCA patients, high ANXA10 expression was confirmed as an independent prognostic factor($P = .026$ in PHCCA, $P = .002$ in DCCA, Cox-regression hazard model). The risk of cancer-caused death in patients with high ANXA10 expression was 2.25- and 3.20-fold higher than in those with low ANXA10 expression.

3.3. ANXA10 promotes the progression of CCA cells in vitro and in vivo

Endogenous ANXA10 expression was detected in the PHCCA cell lines QBC-939 and FRH-0201, as well as in the IHCCA cell lines RBE and HCCC-9810, by qRT-PCR and western blotting (Fig. 2a and b). QBC-939 cells had the highest ANXA10 expression and were thus used as the cell model for RNA knockdown (Fig. 2c and d). CCK-8 assay was applied to detect QBC939 cell proliferation and revealed that ANXA10 knockdown substantially impaired PHCCA cell proliferation (Fig. 2e). Cell cycle and apoptosis in QBC939 cells were detected by flow cytometry (Supplemental Fig. S2a and S2b), but there was no remarkable difference on cell cycle, apoptosis and necrosis between the scrambled and siANXA10 groups (Fig. 2f and g, Supplemental Fig. S2c). Wound healing and transwell assays were also performed to detect the effect of ANXA10 on cell migration (Fig. 2h and i). In our study, ANXA10 knockdown notably attenuated the migration and invasion of QBC939 cells. Similar results were also observed for cell invasion with the Matrigel transwell assay (Fig. 2j). All these results indicated that ANXA10 played an essential role in the invasion and metastasis of PHCCA.

Furthermore, in vivo experiments were performed to evaluate the oncogenic function of ANXA10. First, the stable cells with ANXA10 knockdown were established via infection with a lentivirus carrying ANXA10 shRNA and verified by qRT-PCR and western blotting (Fig. 3a and b). Stable cells were injected subcutaneously into BALB/c nude mice to create xenograft tumors (Fig. 3c). Consequently, ANXA10 knockdown significantly decreased the tumor volumes (Fig. 3d) as well as the tumor weights (Fig. 3e). We futher confirmed the successful

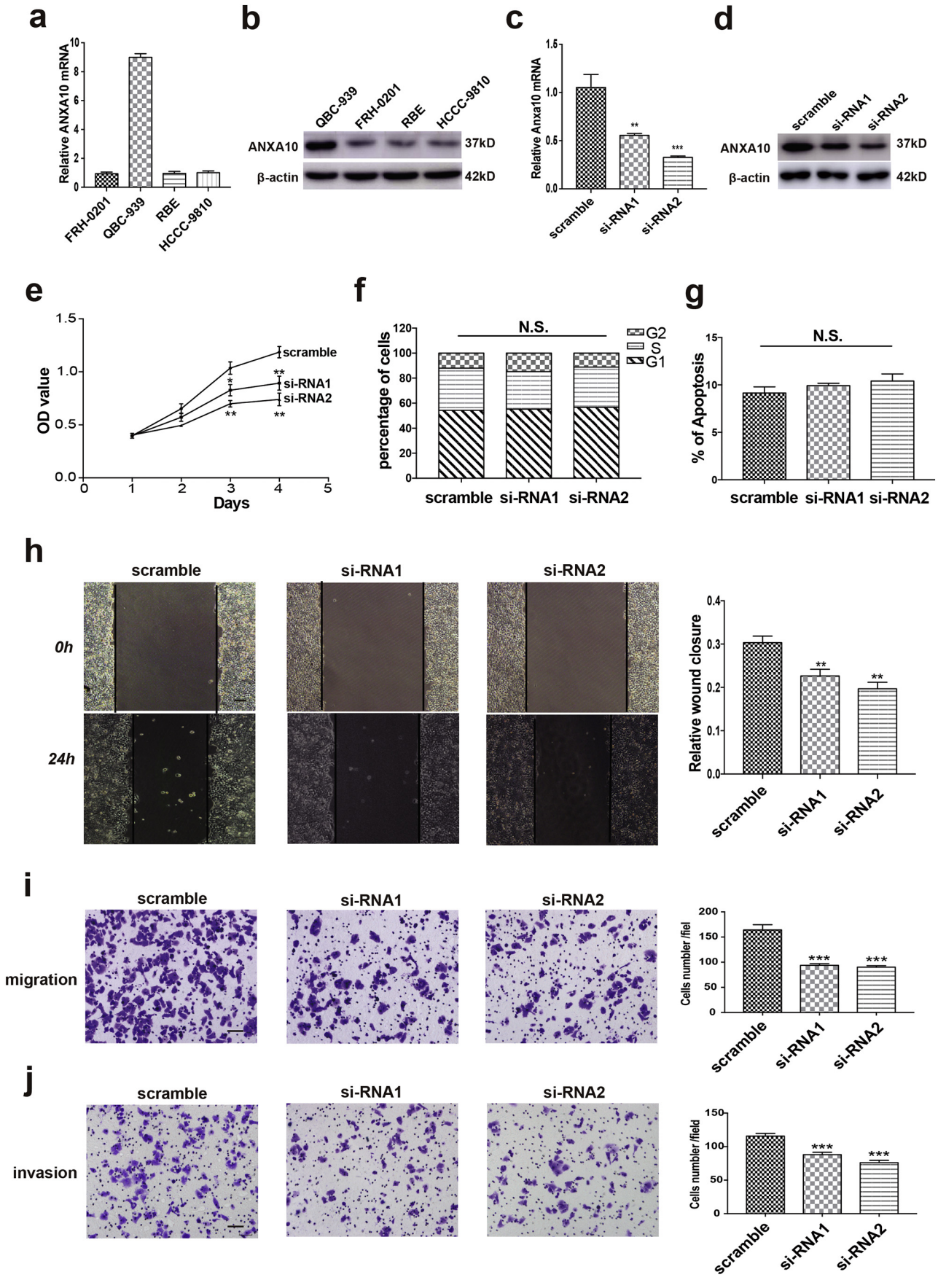
a
Relative ANXA10 mRNA
FRH-0201
QBC-939
RBE
HCCC-9810
b
QBC-939
FRH-0201
RBE
HCCC-9810
ANXA10
37kD
β-actin
42kD
c
Relative Anxa10 mRNA
scramble
si-RNA1
si-RNA2
d
scramble
si-RNA1
si-RNA2
ANXA10
37kD
β-actin
42kD
e
OD value
Days
scramble
si-RNA1
si-RNA2
f
N.S.
percentage of cells
G2
S
G1
scramble si-RNA1 si-RNA2
g
N.S.
% of Apoptosis
scramble si-RNA1 si-RNA2
h
scramble
si-RNA1
si-RNA2
0h
24h
Relative wound closure
i
migration
scramble
si-RNA1
si-RNA2
Cells number /fiel
j
invasion
scramble
si-RNA1
si-RNA2
Cells number /field

long-term ANXA10 knockdown of the xenograft tumors(Supplemental Fig. S3).

Tail vein injection with ANXA10-silenced QBC939 cells was carried out to create tumor metastatic mouse models. The weights of mice injected with shANXA10 were greater than those of mice injected with scrambled shRNA (Fig. 3f), reflecting that ANXA10 knockdown attenuated the systemic metastasis of PHCCA. Tumor metastasis was monitored by in vivo fluorescence imaging (Fig. 3g) and finally confirmed with HE staining and CK19 staining(Fig. 3h and i, supplemental Fig. S4). In our study, ANXA10 silencing strikingly decreased the number of metastatic lesions (Fig. 3j and k), suggesting the important role of ANXA10 in CCA metastasis.

3.4. ANXA10 expression is associated with tumor differentiation and EMT in EHCCA

As shown in Table 1, we observed that ANXA10 expression was significantly associated with PHCCA and DCCA tumor differentiationDCCA, so we further stratified the tumors according to tumor differentiation and ANXA10 expression in PHCCA and DCCA (Fig. 4a and b). For both PHCCA and DCCA, poorly differentiated tumors had higher ANXA10 expression than the moderately and well-differentiated tumors (Fig. 4c and d). Given that EMT is a critical event involved in tumor differentiation and metastasis, the effect of ANXA10 on EMT was measured by detecting EMT-specific proteins, including E-cadherin, Snail and Vimentin. Both qRT-PCR and western blot assays showed increased expression of E-cadherin and decreased expression of Snail and Vimentin after ANXA10 knockdown (Fig. 4e and f), suggesting that ANXA10 was essential for EMT in QBC939 cells.

3.5. PLA2G4A is a key molecule in ANXA10-induced EMT and metastasis

To investigate the downstream targets of ANXA10-induced metastasis of PHCCA and DCCA, transcriptome sequencing was performed (GSE132279), and several significantly altered and metastasis-involved genes (fold change>1.5) were selected (Fig. 5a). Of the altered genes, the enriched genes were clustered into several key signal transduction pathways, and the phospholipase metabolic pathway was the most significantly downregulated pathway after silencing ANXA10 (Fig. 5b). Combined with the above results, 27 genes were chosen for further verification by qRT-PCR (Fig. 5c). The results suggested PLA2G4A and GNA13 as possible targets of ANXA10 (fold change>2.0). Western blotting further demonstrated that the expression of PLA2G4A but not GNA13 was regulated by ANXA10 (Fig. 5d, Supplemental Fig. S5a and S5b). Moreover, PLA2G4A and ANXA10 also exhibited a strong correlation according to exome and transcriptome sequencing (Fig. 1a).

The correlation between ANXA10 and PLA2G4A mRNA was evaluated in 10 cases of PHCCA and DCCA (Fig. 5e), and PLA2G4A expression in 128 PHCCA patients and 84 DCCA patients was detected by IHC (Fig. 5f and g). These results suggested that PLA2G4A expression was significantly associated with ANXA10 in both PHCCA and DCCA. Additionally, the prognostic values of PLA2G4A in PHCCA and DCCA were evaluated with the Kaplan-Meier method. High PLA2G4A expression was also correlated with low overall survival rate in PHCCA and DCCA (Fig. 5h). We combined the ANXA10 and PLA2G4A expression and evaluated the prognostic value of the co-expression of ANXA10 and PLA2G4A. Patients with the co-expression of ANXA10 and PLA2G4A seemed to have poorer prognosis than other patients, suggesting that co-expression of ANXA10 and PLA2G4A may be a more sensitive factor of EHCCA(Fig. 5i).

The role of PLA2G4A in CCA metastasis was investigated because PLA2G4A was previously reported to promote the invasion of several types of cancer [23,24]. A specific inhibitor of PLA2G4A, AACOCT3, was used to suppress PLA2G4A activity after ANXA10 overexpression. Consequently, ANXA10 overexpression promoted EMT (increased Snail and Vimentin and decreased E-cadherin levels) in QBC-939 cells, whereas the PLA2G4A inhibitor partially abolished these changes (Fig. 6a). Moreover, AACOCT3 (20 μM) substantially decreased PLA2G4A-induced QBC939 cell invasion (Fig. 6b and c), suggesting that PLA2G4A was the key effector in ANXA10-mediated invasion and metastasis. A mouse metastasis model was established with stable ANXA10-overexpressing QBC939 cells and treatment with or without AACOCF3. The weights of mice with AACOCF3 treatment were heavier than those without AACOCF3 treatment (Fig. 6d). Metastatic lesions in the liver and lungs were monitored by an in vivo fluorescence system and confirmed with HE (Fig. 6e and f). AACOCF3 notably decreased the number of metastatic lesions in the liver and lungs (Fig. 6g and h). All these results indicated the essential role of PLA2G4A in ANXA10-mediated EMT and metastasis.

3.6. ANXA10 mediates CCA metastasis by activating the PLA2G4A/PGE2/STAT3 pathway

Considering that PGE2 is a primary product of PLA2G4A and a critical cytokine involved in inflammation and tumor metastasis [23], the role of PGE2 in ANXA10-induced invasion and metastasis was further evaluated with in vitro and in vivo experiments. Celecoxib is a well-known specific COX-2 inhibitor that can decrease PGE2 synthesis by inhibiting COX-2. A Matrigel transwell assay revealed that celecoxib (20 μM) significantly attenuated the ANXA10-induced invasion of QBC939 cells (Fig. 7a). In vivo experiments with mice injected with ANXA10-overexpressing QBC939 cells also demonstrated that celecoxib reduced the weight loss induced by ANXA10 overexpression (Fig. 7b) and decreased the number of metastatic lesions in the lungs and livers (Fig. 7c and d). All of the above results suggested that the COX-2 inhibitor celecoxib suppressed the ANXA10-induced invasion and metastasis of EHCCA.

A previous study reported that PEG2 could promote tumor cell invasion and metastasis by activating STAT3 [25]. In our study, we also demonstrated that ANXA10 knockdown decreased while ANXA10 overexpression increased the phosphorylation of STAT3 (Fig. 7e). PGE2 is the primary product of PLA2G4A and COX-2, so exogenous PEG2 at different concentrations was used to stimulate QBC939 cells. PGE2 increased the phosphorylation of STAT3 in a time-dependent manner (Fig. 7f). In addition, ANXA10 overexpression increased STAT3 phosphorylation, while celecoxib inhibited STAT3 phosphorylation and the EMT process in QBC939 cells, suggesting that STAT3

Fig. 2. ANXA10 promotes EHCCA cell proliferation, migration and invasion in vitro. (a and b) ANXA10 expression levels in the human PHCCA cell lines QBC-939 and FRH-0201 and in the IHCCA cell lines RBE and HCCC-9810 were detected by qRT-PCR (a) and western blot. (c and d) Successful knockdown of ANXA10 using two independent siRNAs in QBC-939 cells was verified by qRT-PCR (c) and western blot (d). (e) CCK-8 assays were performed to identify proliferation after ANXA10 knockdown in QBC-939 cells. (f and g) The effect of ANXA10 on the cell cycle (f) and apoptosis (g) was detected with flow cytometry after ANXA10 knockdown in QBC-939 cells. (h) Wound healing assays were performed to identify migration after ANXA10 knockdown in QBC-939 cells. Left: Cells transfected with scrambled siRNA or siANXA10 were cultured for 24 h after scratching. Right: The percentage of wound closure for cells with scrambled siRNA and siANXA10. Scale bar: 100 μm. (i) Transwell assays without Matrigel were used to evaluate the migration of QBC-939 cells after ANXA10 knockdown. Left: Representative images of migrated cells. Right: The statistical number of migrated cells with scrambled siRNA and siANXA10. Scale bar: 50 μm. (j) Transwell assays with Matrigel were used to evaluate the invasion of QBC-939 cells. In e–j, statistical significance between subgroups was assessed with Student's *t*-test. N.S. means not significant; *, ** and *** represent $p < .05$, $p < .01$ and $p < .001$, respectively.

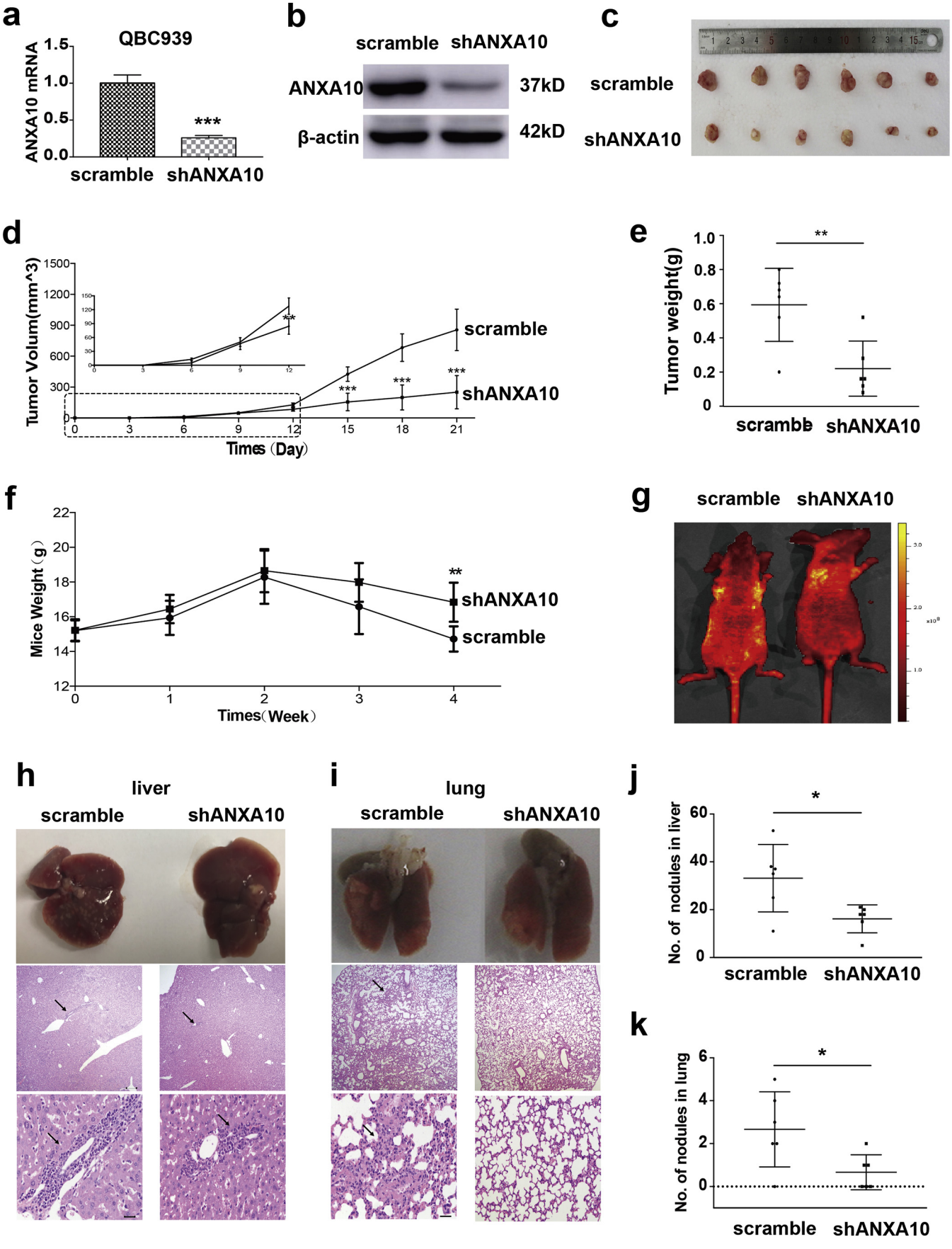
a
QBC939
ANXA10 mRNA
1.5
1.0
0.5
0.0
***
scramble
shANXA10
b
scramble
shANXA10
ANXA10
37kD
β-actin
42kD
c
scramble
shANXA10
d
Tumor Volum(mm^3)
1500
1200
900
600
300
0
0
3
6
9
12
15
18
21
**
***
scramble
shANXA10
Times (Day)
e
Tumor weight(g)
1.0
0.8
0.6
0.4
0.2
0
**
scramble
shANXA10
f
Mice Weight (g)
22
20
18
16
14
12
0
1
2
3
4
**
shANXA10
scramble
Times(Week)
g
scramble
shANXA10
h
liver
scramble
shANXA10
i
lung
scramble
shANXA10
j
No. of nodules in liver
60
40
20
0
*
scramble
shANXA10
k
No. of nodules in lung
6
4
2
0
*
scramble
shANXA10

phosphorylation was required for ANXA10/ PLA2G4A-induced EMT and metastasis.

4. Discussion

Although the ANXA family members are known to have essential functions, including cell division, growth regulation, vesicle trafficking and calcium signaling, the role of the ANXA family in tumorigenesis and tumor progression is still controversial. As a new member of the ANXA family, studies on ANXA10 in cancer progression are rare and sporadic. For the first time, we screened ANXA10 by mRNA sequencing and identified it as a prognostic biomarker of PHCCA and DCCA, but not ICCA. Since CCA specimens are difficult to obtain, the cohort sample size (91 ICCA, 128 PHCCA and 84 DCCA tissues) in our study was large, and we provided remarkable statistical significance suggesting ANXA10 as a prognostic biomarker. Our results suggested that pathological detection of ANXA10 would help stratify patients with EHCCA more precisely. Patients with high ANXA10 expression are high risk and may suffer an unfavorable prognosis, which may provide important information for the individualized treatment of EHCCA. Moreover, we demonstrated that ANXA10 predicted poor prognosis in PHCCA and DCCA but not in IHCCA. This finding was also a supportive evidence of that ICCA and EHCCA had different molecular and biological features.

The physiological function of ANXA10 has not been well studied, and the underlying mechanism of how ANXA10 correlates with tumor progression is far from clear. In our study, we demonstrated for the first time that ANXA10 promoted the invasion and metastasis of EHCCA by facilitating EMT. Moreover, we suggested that ANXA10 promoted PLA2G4A expression and thus increased PGE2 generation and activated STAT3, thereby promoting EMT. These findings greatly supplement our knowledge of the oncogenic role of ANXA10 and even the whole ANXA family. Interestingly, the most well-known ANXA family member, ANXA1, was demonstrated to inhibit PLA2 activity and thereby blocking eicosanoid production[14,15], but we showed that ANXA10 promoted the expression of PLA2 in our study, which has not been reported about the ANXA family. Considering that the functions of ANXA family members are notably tissue-specific and context-specific, it is also possible that ANXA10 and ANXA1 exhibit different regulations of PLA2 expression and activity in different tumor types or pathological processes.

Our results demonstrated that the ANXA10-induced PLA2G4A/COX-2/PEG2/STAT3 pathway played an important role in EHCCA metastasis and indicated that blocking this pathway may be a promising therapeutic approach to treat EHCCA. In fact, the anti-tumor effects of non-steroidal anti-inflammatory drugs (NSAIDs) have attracted great attention for a long time because inflammation is a recognized hallmark of cancer that continuously contributes to the development and progression of malignancies. For example, aspirin treatment was associated with a reduction of morbidity in patients with colorectal adenoma [26,27], and NSAIDs were reported to improve patient survival for PIK3CA-altered head and neck cancer [28]. Regarding CCA, aspirin use was demonstrated to decrease the risk for all the three CCA subtypes [29]. The molecular mechanisms of how NSAIDs suppress tumor progression have also been widely examined in previous studies [30]. One important explanation is that NSAIDs reduce AA and PGE2 generation and therefore inhibite PGE2-induced tumor progression, which was also supported by our results. In our study, we furthermore proved that PGE2 promoted EMT and facilitated metastasis via activating STAT3 in QBC939 cells with multiple in vivo experiments. EMT is the key process of ANXA10-mediating metastasis of EHCCA since EMT makes cancer cells more aggressive, resistant to apoptosis and confers stem-like features. Moreover, EMT programs can promote the production of inflammation factors by cancer cells. In our study, the close correlation between PLA2G4A/COX-2/PGE2 and EMT in EHCCA indicated that inflammation and EMT may sustain each other in EHCCA, and that the inflammation-EMT axis plays a significant role in CCA metastasis. This should be paid more attention because longstanding inflammation is inevitable because of the bilioenteric anastomosis and bacterial influx after radical surgery for PHCCA or DCCA. In our previous study, we also demonstrated that biliary inflammation correlated with the recurrence of PHCCA by promoting HMGB1 release [6].

Because of the low incidence and high difficulty of radical surgery, DCCAthe potential biomarkers, genetic alterations, and targeted drugs in preclinical studies or clinical trials for PHCCA and DCCA are far behind other common cancer types, such as lung cancer or colon cancer. Even IHCCA studies have made great progresses in molecular classification and genetic alteration screening, but studies of targeted therapy for PHCCA and DCCA have remained stagnant in recent years. Our results indicated that PLA2G4A and its downstream targets COX-2, PGE2 and STAT3 can all be regarded as potential drug targets for PHCCA and DCCA. PLA2G4A, COX-2, and PGE2 have all been demonstrated to be involved in the progression and prognosis of many types of cancers, including breast cancer, ovarian cancer and hepatocellular carcinoma [31–33]. COX-2 is a potential drug target for several types of cancers, and COX-2 inhibitors are extensively used to treat inflammation and exhibit anti-tumor effect in numerous studies. Our results demonstrated that PLA2G4A and downstream PGE2 promoted the metastasis of EHCCA via facilitating EMT, and indicated that inhibitors of PLA2G4A and COX-2 suppressed ANXA10-induced metastasis. These results revealed new molecular mechanism of EHCCA metastasis and provided new insights into precise treatment of PHCCA and DCCA. Our findings pointed the potency of NSAIDs as promising drug to suppress metastasis of PHCCA and DCCA.

In conclusion, we first demonstrated that ANXA10 is an independent prognostic biomarker of PHCCA and DCCA. After various in vitro and in vivo experiments, we suggested that PLA2G4A expression was regulated by ANXA10 and that it is essential for ANXA10-induced proliferation, invasion and EMT in CCA. PGE2 generation and STAT3 activation downstream of PLA2G4A led to ANXA10-mediated EMT facilitation and tumor metastasis. Our results may help stratify high-risk patients with PHCCA and DCCA and guide individualized treatment for PHCCA and DCCA. ANXA10, PLA2G4A and COX-2 are potential drug targets for PHCCA and DCCA, and blocking the ANXA10/PLA2G4A/PGE2 pathway is a promising therapeutic approach for CCA treatment.

Funding

Our study was supported by National Natural Science Foundation of China (Grant no. 81601668), Shandong Province Major Research and Design Program (Grant No. 2018GSF118169), Jinan City Science and Technology Development Program (Grant No. 201805017, 201805013), and Hengrui Hepatobiliary and Pancreatic Foundation (Grant No·Y-2017-144).

Fig. 3. ANXA10 promotes EHCCA cell proliferation and metastasis in vivo. (a and b) Stable QBC939 cells with ANXA10 knockdown were verified by qRT-PCR (a) and western blot (b). (c) Subcutaneous xenograft tumors in nude mice were established with stable QBC939 cells with shANXA10 or scrambled shRNA. (e and e) The volumes and weights were lower for xenograft tumors with ANXA10 knockdown than for xenograft tumors with scrambled shRNA. (f) A metastatic model was established by caudal vein injection of QBC939 cells and monitored by a live fluorescence system. (g) Mice injected with ANXA10-silenced QBC939 cells had heavier body weights than control mice. (h and i) Representative gross specimens and HE staining of metastatic lesions in the liver (h) and lungs (i). The arrows indicate the metastatic lesions. Scale bar: 20 μm. (j and k) The number of metastases on the surfaces of livers (j) and lungs (k) is counted in the bottom panel. In a, e, g, j and k, the statistical significance between the scrambled and shANXA10 groups was assessed using Student's t-test. *, ** and *** represent $p < .05$, $p < .01$ and $p < .001$, respectively.

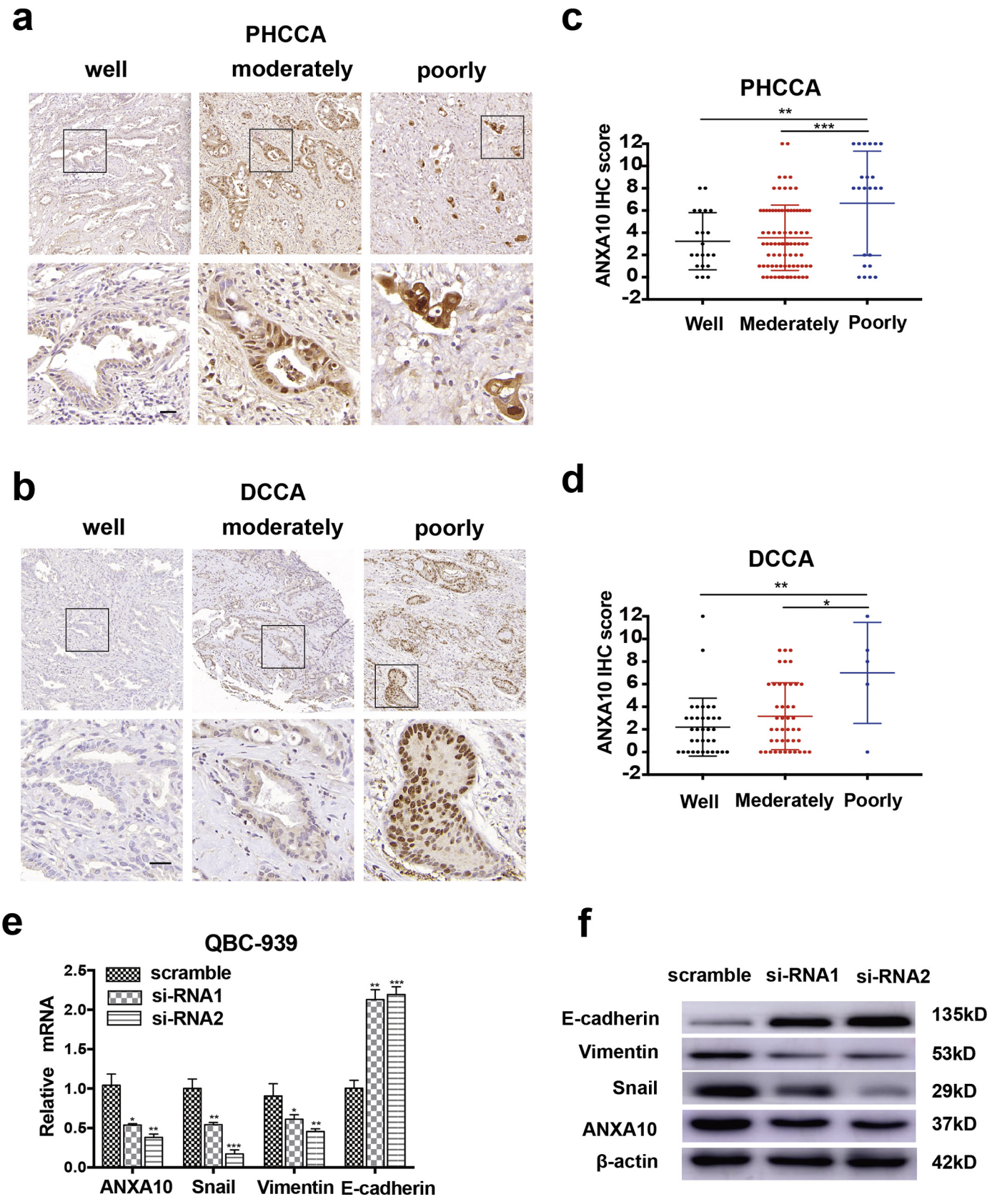

Fig. 4. ANXA10 expression was associated with tumor differentiation and EMT in EHCC. (a–d) Representative IHC staining (a and b) and score for ANXA10 (c and d) in well, moderately and poorly differentiated PHCCA and DCCA. Scale bar: 50 μm. (e and f) Changes in the expression of the EMT biomarkers Snail, Vimentin and E-cadherin after ANXA10 knockdown were detected by qRT-PCR (e) and western blot (f). Statistical significance between groups was assessed using Student's t-test. *, ** and *** represent $p < .05$, $p < .01$ and $p < .001$, respectively.

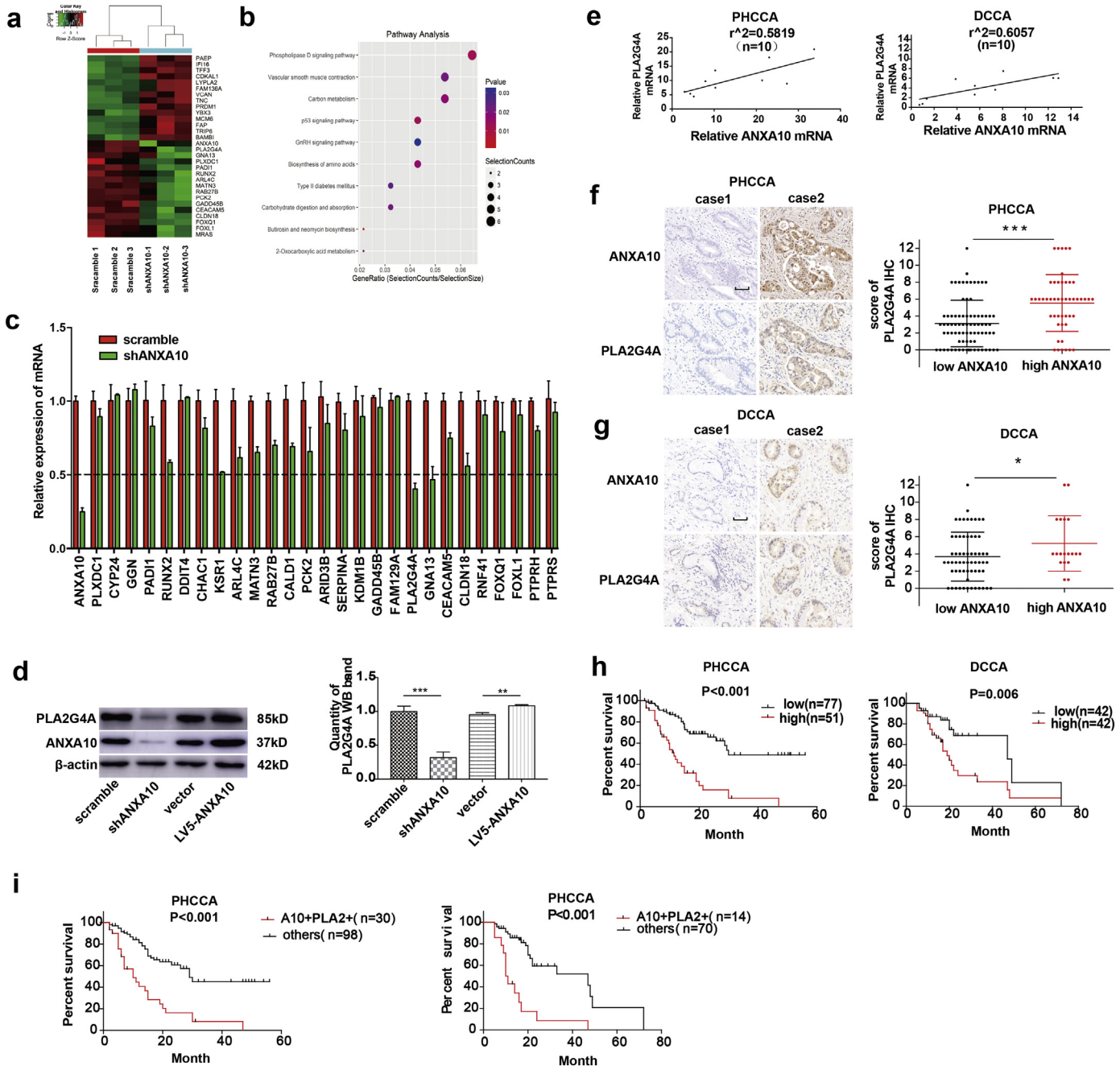

Fig. 5. PLA2G4A is a downstream target of ANXA10 in EHCC. (a) Heatmap of distinctly dysregulated mRNAs in stable QBC-939 cell lines (scrambled shRNA vs shANXA10) identified from transcriptome sequencing by hierarchical clustering. High and low expression levels are indicated in red and green, respectively. (b) Pathway analysis of distinctly dysregulated pathways in stable QBC-939 cell lines identified from exon and transcriptome sequencing. Statistical significance is indicated by different colors. The size of the circle represents the number of genes in each pathway. (c) The mRNA levels of 27 candidate genes in QBC939 cells with ANXA10 knockdown were detected by qRT-PCR. (d) PLA2G4A expression was regulated by ANXA10. Left: PLA2G4A expression in QBC939 cells was detected by western blot after ANXA10 knockdown or overexpression. Right: Quantification of ANXA10 expression in the left panel. (e) The association between relative PLA2G4A and ANXA10 mRNA levels in 10 PHCCA and DCCA fresh tissue samples was analyzed according to the Pearson-correlation factor. (f–g) PHCCA and DCCA patients with high ANXA10 expression also had high PLA2G4A expression. Left: Representative IHC images of ANXA10 expression in PHCCA (f) and DCCA (g). Scale bar: 50 μm. Right: IHC score of PLA2G4A for PHCCA (f) and DCCA (g) patients with low or high ANXA10 expression. Statistical significance between groups was assessed using Student's t-test. * represents $p < .05$. (h) Overall survival curves for patients with PHCCA and DCCA were stratified according to PLA2G4A expression. (i) Overall survival curves for patients with PHCCA and DCCA were stratified according to patients with co-expression of ANXA10 and PLA2G4A, and other patients.

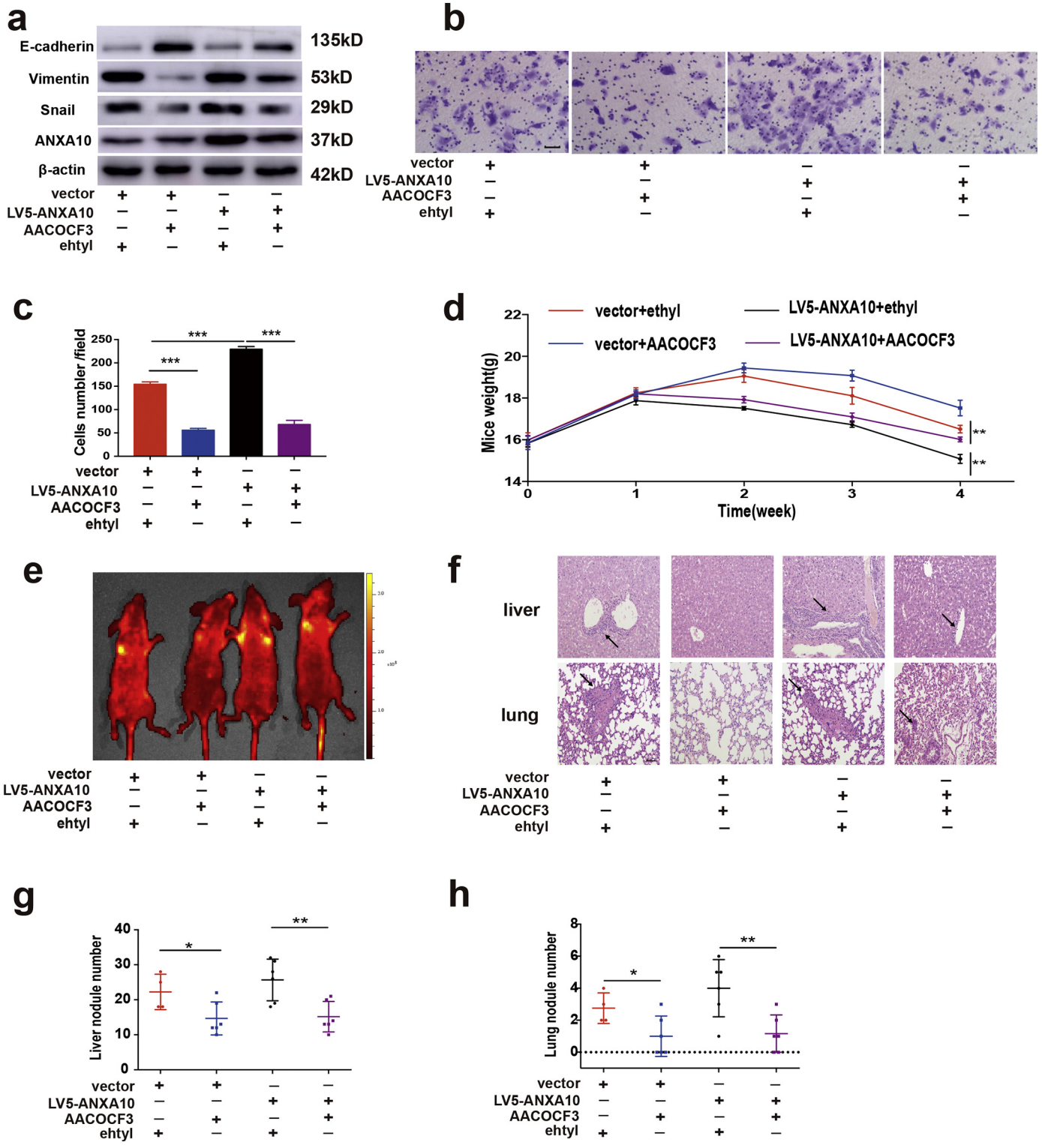

Fig. 6. PLA2G4A is required for ANXA10-induced EHCCA metastasis. (a) Changes in EMT biomarker expression, including Snail, Vimentin and E-cadherin, were detected in ANXA10-overexpressing QBC939 cells with or without AACOCT3 (20 μM) incubation for 48 h. (b) Representative images of invaded ANXA10-overexpressing QBC939 cells in the presence or absence of 20 μM AACOCT3 for 24 h. Scale bar: 50 μm. (c) Numbers of invaded QBC939 cells transfected with empty vector or LV5-ANXA10. (d) Body weights of the mouse metastatic models injected with ANXA10-overexpressing QBC939 cells and treated with or without AACOCT3. (e) Metastases of stable QBC939 cells overexpressing ANXA10 and treated with/without AACOCF3 (10 mg/kg) were monitored by in vivo fluorescence imaging systems. (f) Metastatic lesions in the livers (e) and lungs (f) were confirmed by HE staining (400 × magnification). The arrows indicate metastatic lesions. Scale bar: 50 μm. (g and h) The number of metastases on the surfaces of the livers and lungs was quantified.

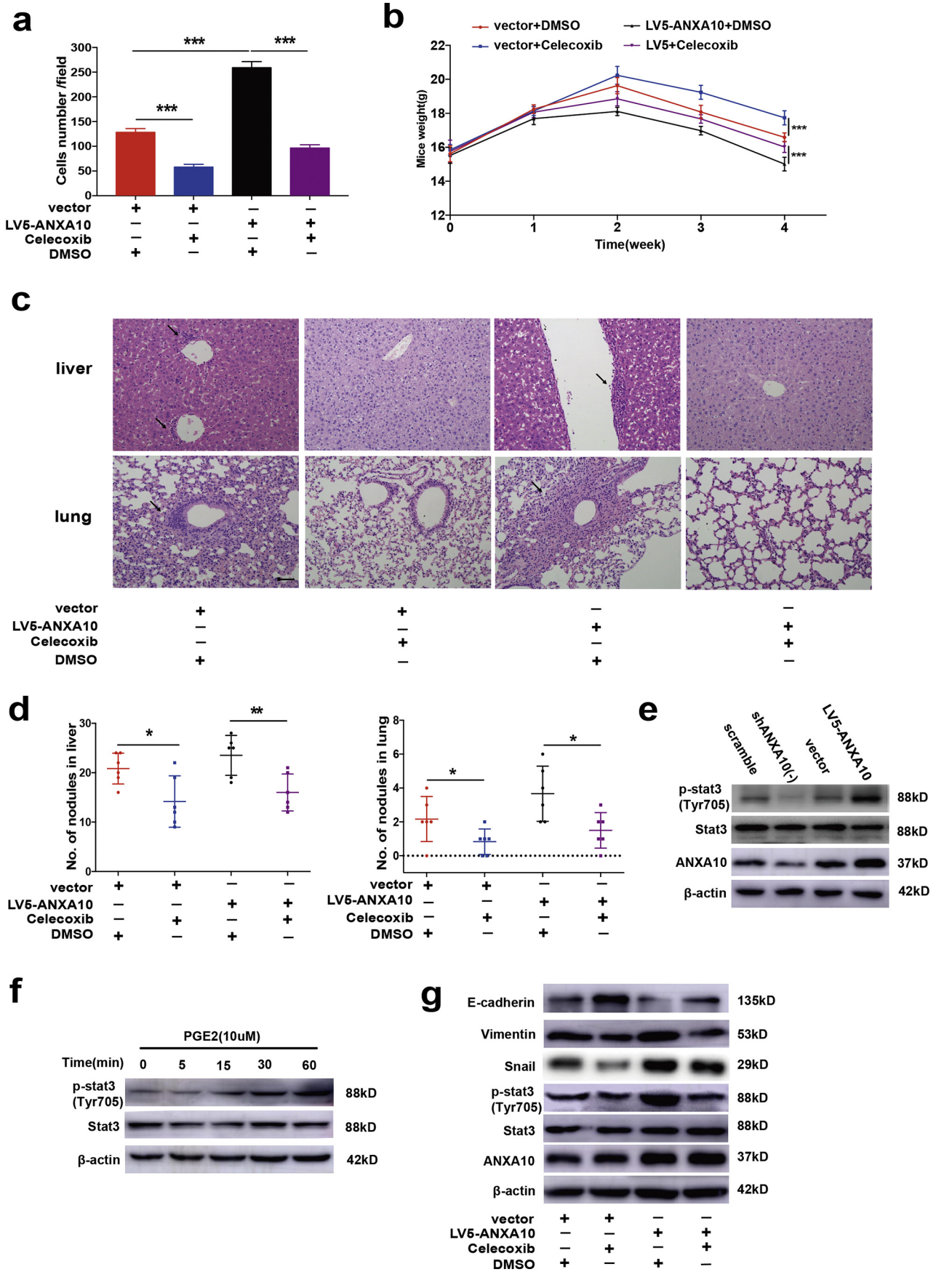

Fig. 7. ANXA10 mediates the migration of EHCC cells through the PLA2G4A/PGE2/STAT3 pathway. (a) The COX2 inhibitor celecoxib decreased the invasion induced by ANXA10 overexpression. (b) The weights of mice injected with ANXA10-overexpressing QBC939 cells and treated with or without celecoxib (200 mg/kg) were measured every week. (c) Metastatic lesions in the liver and lungs were confirmed with HE staining under 400× magnification. Scale bar: 50 μm. (d) The number of metastases on the surfaces of the livers and lungs was quantified from (c). (e) The effects of ANXA10 on STAT-3 phosphorylation were detected by western blotting. (f) Time response of exogenous PGE2 to STAT-3 phosphorylation in QBC939 cells. (g) Expression changes in EMT biomarkers after ANXA10 overexpression with or without celecoxib (20 μM) incubation for 48 h.

Author contributions

S. RQ, Q.B, L. ZL, Z. XM, C. TL and L. ZP carried out experiments. Z.ZL collected the samples. X. YF and Z. ZL. analyzed data. X. YF conceived experiments and wrote the paper. All authors had final approval of the submitted and published versions.

Declaration of Competing Interest

We declare no conflicts of interests.

Acknowledgments

We thank Dr. Xiaoqing Yang from the Department of Pathology, the Qianfoshan Hospital of Shandong University, for evaluating the results of immunohistochemistry.

Appendix A. Supplementary data

Supplementary data to this article can be found online at https://doi.org/10.1016/j.ebiom.2019.08.062.

References

[1] Squadroni M, Tondulli L, Gatta G, Mosconi S, Beretta G, Labianca R. Cholangiocarcinoma. Crit Rev Oncol Hematol 2017;116:11–31 [Epub 2017/07/12].
[2] Xu YF, Yang XQ, Lu XF, Guo S, Liu Y, Iqbal M, et al. Fibroblast growth factor receptor 4 promotes progression and correlates to poor prognosis in cholangiocarcinoma. Biochem Biophys Res Commun 2014;446(1):54–60 [Epub 2014/02/26].
[3] Rizvi S, Khan SA, Hallemeier CL, Kelley RK, Gores GJ. Cholangiocarcinoma - evolving concepts and therapeutic strategies. Nat Rev Clin Oncol 2018;15(2):95–111 [Epub 2017/10/11].
[4] Razumilava N, Gores GJ. Cholangiocarcinoma Lancet 2014;383(9935):2168–79 [Epub 2014/03/04].
[5] Blechacz B. Cholangiocarcinoma: current knowledge and new developments. Gut Liver 2017;11(1):13–26 [Epub 2016/12/09].
[6] Xu YF, Liu ZL, Pan C, Yang XQ, Ning SL, Liu HD, et al. HMGB1 correlates with angiogenesis and poor prognosis of perihilar cholangiocarcinoma via elevating VEGFR2 of vessel endothelium. Oncogene 2019;38(6):868–80 [Epub 2018/09/05].
[7] Shinohara K, Ebata T, Shimoyama Y, Mizuno T, Yokoyama Y, Yamaguchi J, et al. A study on radial margin status in resected Perihilar cholangiocarcinoma. Ann Surg 2019. https://doi.org/10.1097/SLA.0000000000003305 [Epub 2019/04/05].
[8] Yang XQ, Xu YF, Guo S, Liu Y, Ning SL, Lu XF, et al. Clinical significance of nerve growth factor and tropomyosin-receptor-kinase signaling pathway in intrahepatic cholangiocarcinoma. World J Gastroenterol 2014;20(14):4076–84 [Epub 2014/04/20].
[9] Liu Z, Sun R, Zhang X, Qiu B, Chen T, Li Z, et al. Transcription factor 7 promotes the progression of perihilar cholangiocarcinoma by inducing the transcription of c-Myc and FOS-like antigen 1. EBioMedicine 2019;45:181–91 [Epub 2019/06/30].
[10] Rizvi S, Gores GJ. Emerging molecular therapeutic targets for cholangiocarcinoma. J Hepatol 2017;67(3):632–44 [Epub 2017/04/09].
[11] Mussunoor S, Murray GI. The role of annexins in tumour development and progression. J Pathol 2008;216(2):131–40 [Epub 2008/08/14].
[12] Gerke V, Moss SE. Annexins: from structure to function. Physiol Rev 2002;82(2):331–71 [Epub 2002/03/28].
[13] Pessolano E, Belvedere R, Bizzarro V, Franco P, Marco I, Porta A, et al. Annexin A1 may induce pancreatic Cancer progression as a key player of extracellular vesicles effects as evidenced in the in vitro MIA PaCa-2 model system. Int J Mol Sci 2018;19(12) [Epub 2018/12/07].
[14] Yi M, Schnitzer JE. Impaired tumor growth, metastasis, angiogenesis and wound healing in annexin A1-null mice. Proc Natl Acad Sci U S A 2009;106(42):17886–91 [Epub 2009/10/07].
[15] Srivastava M, Bubendorf L, Srikantan V, Fossom L, Nolan L, Glasman M, et al. ANX7, a candidate tumor suppressor gene for prostate cancer. Proc Natl Acad Sci U S A 2001;98(8):4575–80 [Epub 2001/04/05].
[16] Dyson JK, Beuers U, Jones DEJ, Lohse AW, Hudson M. Primary sclerosing cholangitis. Lancet 2018;391(10139):2547–59 [Epub 2018/02/18].
[17] Rizvi S, Gores GJ. Pathogenesis, diagnosis, and management of cholangiocarcinoma. Gastroenterology 2013;145(6):1215–29 [Epub 2013/10/22].
[18] Patel MI, Singh J, Niknami M, Kurek C, Yao M, Lu S, et al. Cytosolic phospholipase A2-alpha: a potential therapeutic target for prostate cancer. Clin Cancer Res 2008;14(24):8070–9 [Epub 2008/12/18].
[19] Kim SW, Rhee HJ, Ko J, Kim YJ, Kim HG, Yang JM, et al. Inhibition of cytosolic phospholipase A2 by annexin I. specific interaction model and mapping of the interaction site. J Biol Chem 2001;276(19):15712–9 [Epub 2001/03/30].
[20] Xu Y, Yang X, Li Z, Li S, Guo S, Ismail S, et al. Sprouty2 correlates with favorable prognosis of gastric adenocarcinoma via suppressing FGFR2-induced ERK phosphorylation and cancer progression. Oncotarget 2017;8(3):4888–900 [Epub 2016/12/22].
[21] Liu H, Xu Y, Zhang Q, Yang H, Shi W, Liu Z, et al. Prognostic significance of TBL1XR1 in predicting liver metastasis for early stage colorectal cancer. Surg Oncol 2017;26(1):13–20 [Epub 2017/03/21].
[22] Liu H, Xu Y, Zhang Q, Li K, Wang D, Li S, et al. Correlations between TBL1XR1 and recurrence of colorectal cancer. Sci Rep 2017;7:44275 [Epub 2017/03/16].
[23] Fu H, He Y, Qi L, Chen L, Luo Y, Li Y, et al. cPLA2alpha activates PI3K/AKT and inhibits Smad2/3 during epithelial-mesenchymal transition of hepatocellular carcinoma cells. Cancer Lett 2017;403:260–70 [Epub 2017/06/27].
[24] Chen L, Fu H, Luo Y, Cheng R, Zhang N, Guo H. cPLA2alpha mediates TGF-beta-induced epithelial-mesenchymal transition in breast cancer through PI3k/Akt signaling. Cell Death Dis 2017;8(4):e2728 [Epub 2017/04/07].
[25] Tong D, Liu Q, Liu G, Xu J, Lan W, Jiang Y, et al. Metformin inhibits castration-induced EMT in prostate cancer by repressing COX2/PGE2/STAT3 axis. Cancer Lett 2017;389:23–32 [Epub 2017/01/04].
[26] Ricciardiello L, Ahnen DJ, Lynch PM. Chemoprevention of hereditary colon cancers: time for new strategies. Nat Rev Gastroenterol Hepatol 2016;13(6):352–61 [Epub 2016/04/21].
[27] Hull MA, Sprange K, Hepburn T, Tan W, Shafayat A, Rees CJ, et al. Eicosapentaenoic acid and aspirin, alone and in combination, for the prevention of colorectal adenomas (seAFOod polyp prevention trial): a multicentre, randomised, double-blind, placebo-controlled, 2 x 2 factorial trial. Lancet 2018;392(10164):2583–94 [Epub 2018/11/24].
[28] Hedberg ML, Peyser ND, Bauman JE, Gooding WE, Li H, Bhola NE, et al. Use of non-steroidal anti-inflammatory drugs predicts improved patient survival for PIK3CA-altered head and neck cancer. J Exp Med 2019;216(2):419–27 [Epub 2019/01/27].
[29] Altaii H, Al-Kindi SG, Oliveira GH, Yaqoob Z, Romero-Marrero C. Aspirin use and risk of cholangiocarcinoma: external validation with big data. Hepatology 2017;65(4):1421–2 [Epub 2017/01/05].
[30] Patrignani P, Patrono C. Aspirin and Cancer. J Am Coll Cardiol 2016;68(9):967–76 [Epub 2016/08/27].
[31] Schulte RR, Linkous AG, Hallahan DE, Yazlovitskaya EM. Cytosolic phospholipase A2 as a molecular target for the radiosensitization of ovarian cancer. Cancer Lett 2011;304(2):137–43 [Epub 2011/03/15].
[32] Caiazza F, McCarthy NS, Young L, Hill AD, Harvey BJ, Thomas W. Cytosolic phospholipase A2-alpha expression in breast cancer is associated with EGFR expression and correlates with an adverse prognosis in luminal tumours. Br J Cancer 2011;104(2):338–44 [Epub 2010/12/02].
[33] Alimirah F, Peng X, Yuan L, Mehta RR, von Knethen A, Choubey D, et al. Crosstalk between the peroxisome proliferator-activated receptor gamma (PPARgamma) and the vitamin D receptor (VDR) in human breast cancer cells: PPARgamma binds to VDR and inhibits 1alpha, 25-dihydroxyvitamin D3 mediated transactivation. Exp Cell Res 2012;318(19):2490–7 [Epub 2012/08/14].